Modelling and simulation analysis of a direct-drive system for specific motion laws of the heald frame

DOI: 10.35530/IT.077.04.2025112

QINGYUAN GUO
TAO YANG
SIJIA FU
HONGBIN YU

ABSTRACT – REZUMAT

Modelling and simulation analysis of a direct-drive system for specific motion laws of the heald frame

This study presents a modelling and simulation analysis of a direct-drive system for the heald frame in looms, utilising an 11th-order polynomial to achieve smooth, continuous motion with C^3 continuity in displacement, velocity, and acceleration. A d-q axis mathematical model based on electromagnetic-mechanical coupling is established, and Clark-Park transformation enables decoupled control of flux and thrust. Simulations in MATLAB/Simulink under varying heald frame masses (2.5–10 kg) show linear increases in load force (±3.8 to ±15.2 N), q-axis current (±25 to ±90 mA), and electromagnetic thrust (±7.6 to ±30.3 N), with stable three-phase currents and rapid, overshoot-free response. Results validate the model's accuracy and the effectiveness of the control strategy, demonstrating excellent dynamic performance, load adaptability, and energy efficiency. The direct-drive system eliminates mechanical transmission losses, offering a foundation for high-precision, green weaving technology.

Keywords: *heald frame, direct-drive system, motion control, electromechanical coupling modelling, motion law, electromagnetic thrust*

Analiza modelării și simulării unui sistem cu acționare directă pentru legi specifice de mișcare ale ițelor

Prezentul studiu prezintă o analiză de modelare și simulare a unui sistem de acționare directă pentru mașinile de țesut cu ițe, utilizând un polinom de ordinul 11 pentru a obține o mișcare lină și continuă, cu continuitate de tip C^3 în ceea ce privește deplasarea, viteza și accelerația. Se elaborează un model matematic pe axele d-q bazat pe cuplajul electromagnetico-mecanic, iar transformarea Clark-Park permite controlul decuplat al fluxului și al forței de împingere. Simulările efectuate în MATLAB/Simulink pentru mase variabile ale ițelor (2,5–10 kg) arată creșteri liniare ale forței de sarcină (de la ±3,8 până la ±15,2 N), ale curentului pe axa q (de la ±25 la ±90 mA) și ale forței de împingere electromagnetică (de la ±7,6 la ±30,3 N), cu curenți trifazici stabili și un răspuns rapid, fără depășiri. Rezultatele validează acuratețea modelului și eficacitatea strategiei de control, demonstrând performanțe dinamice excelente, adaptabilitate la sarcină și eficiență energetică. Sistemul cu acționare directă elimină pierderile de transmisie mecanică, oferind o bază pentru o tehnologie de țesere ecologică și de înaltă precizie.

Cuvinte-cheie: *iță, sistem de acționare directă, controlul mișcării, modelare cuplaj electromecanic, legea mișcării, forță de împingere electromagnetică*

INTRODUCTION

In modern weaving technology, the Heald frame is the core actuating component responsible for the fabric's shedding motion, directly influencing loom efficiency, fabric quality, and equipment stability [1–3]. Traditional high-speed rotary electronic dobby (HRED) machines use conjugate cam-driven crank-rocker mechanisms to convert the main shaft's uniform rotation into variable-speed motion with intermittent pauses, accommodating different fabric structures [4, 5]. However, these mechanical transmission systems suffer from multiple stages, large inertia, slow response, and non-adjustable motion laws, limiting their suitability for high-speed, high-precision applications [6, 7].

Recent research has focused on structural optimisation, motion simulation, and dynamic modelling of dobby machines, laying the groundwork for drive system design [8, 9]. Despite these efforts, traditional mechanical structures remain constrained by inherent performance bottlenecks. With advances in linear drive technology, Permanent Magnet Linear Synchronous Motors (PMLSMs) have emerged as a promising alternative due to their high thrust density, fast response, and precise positioning [10–12]. Studies have explored structural design, electromagnetic optimisation, thrust ripple suppression, and advanced control strategies. For instance, Tan et al. reduced thrust ripple through pole pair optimisation [13], Huang et al. enhanced current control via dead-time compensation [14], Tan et al. improved positioning accuracy using disturbance observers [15], and Zeng et al. optimised motor structures via finite element analysis [16].

Compared to HRED systems, PMLSM-based direct-drive systems offer superior dynamic performance and flexibility. This study presents a mathematical model of a PMLSM direct-drive system tailored to the

Heald frame motion laws, addressing the complex electromechanical coupling characteristics and providing a foundation for advanced control and optimisation.

WORKING PRINCIPLE AND MATHEMATICAL MODEL OF THE DIRECT-DRIVE SYSTEM

Working principle

The heald frame direct-drive system is a novel linear drive system. Its core innovation lies in eliminating the conventional mechanical transmission devices commonly used in traditional looms, and instead adopting electromagnetic driving technology to directly drive the heald frame through electromagnetic thrust, achieving reciprocating vertical motion. This approach realises a highly integrated structural design. The structural diagram is shown in figure 1.

The system mainly consists of a stator winding (primary part), a permanent magnet mover (secondary part), a support and guidance mechanism, and mechanical structures directly connected to the heald frame. Unlike indirect drive systems that rely on intermediate components such as cams or linkages, which introduce backlash, wear, and friction, the direct-drive configuration ensures a one-to-one correspondence between electrical input and mechanical output, enhancing position fidelity and reducing parasitic power losses. The absence of lubricated joints lowers maintenance requirements and avoids contamination [17, 18]. Due to complex electromechanical coupling within the system, a comprehensive mathematical model integrating electromagnetic and mechanical dynamics is essential for developing high-performance control strategies and conducting system performance analysis.

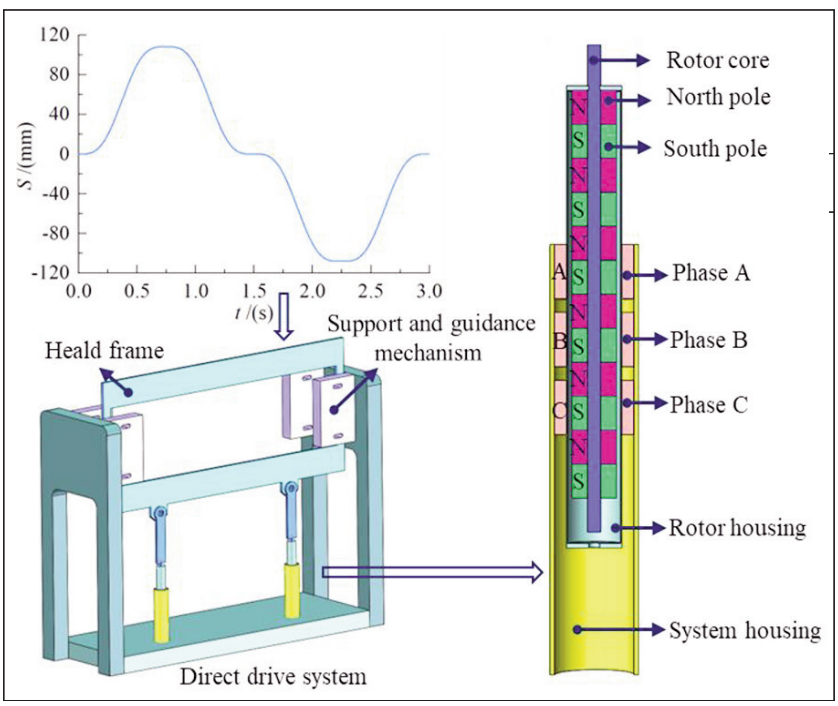

Fig. 1. Schematic diagram of the structure of the direct-drive heald frame system

Mathematical model

An 11th-order polynomial displacement function is designed for the heald frame to ensure smooth motion, continuous acceleration, and stable performance in high-speed weaving, meeting strict requirements for displacement, velocity, and jerk continuity:

$$S = h\begin{pmatrix} 336(\xi)^5 - 1890(\xi)^6 + 4740(\xi)^7 - 6615(\xi)^8 \\ +5320(\xi)^9 - 2310(\xi)^{10} + 420(\xi)^{11} \end{pmatrix} \quad (1)$$

where h is the heald frame lift, and ξ – the angular variable describing the heald frame motion position.

The total load force F_L experienced by the heald frame during motion can be expressed as:

$$F_L = F_e - Bv - ma \quad (2)$$

where m is the equivalent mass of the heald frame, B – the viscous friction coefficient, and a and v are the acceleration and velocity, respectively. The load force F_L reflects the sum of the inertial force and frictional force that must be overcome by the heald frame under different motion states, and serves as an important basis for the design of electromagnetic thrust.

The direct-drive heald frame system efficiently converts electrical energy into mechanical energy to drive the permanent magnet mover in linear reciprocating motion. The three-phase instantaneous power P_{abc}, which is related to the velocity v, reflects the process of electromagnetic thrust generation:

$$P_{abc} = e_a i_a + e_b i_b + e_c i_c =$$
$$= -\phi_f \omega_e \left[i_a \sin\theta_e + i_b \sin\left(\theta_e - \frac{2\pi}{3}\right) + i_c \sin\left(\theta_e + \frac{2\pi}{3}\right)\right]$$

where ϕ_f is the flux linkage produced by the permanent magnet, θ_e is the electrical angle, representing the electrical position of the mover relative to the stator, which affects the back EMF and thrust magnitude. ω_e is the electrical angular velocity.

According to the principle of energy conservation, the electromagnetic thrust F_e generated by the system can be derived from the relationship between instantaneous power and motion velocity. The specific expression is:

$$F_e = \frac{P_{abc}}{v} = \frac{\pi}{\tau_n}\phi_f \left[i_a \sin(-\theta_e) + \right. \quad (4)$$
$$\left. + i_b \sin\left(\theta_e - \frac{2\pi}{3}\right) + i_c \sin\left(\theta_e + \frac{2\pi}{3}\right)\right]$$

where τ_n is the pole pitch.

In order to achieve high-performance control of the direct-drive heald frame system, it is usually necessary to transform the three-phase stationary coordinate system (abc coordinate system) into a two-phase rotating coordinate system (d–q coordinate system), thereby achieving decoupled control of the magnetic field and thrust.

Clark transformation:

$$\begin{bmatrix} i_\alpha \\ i_\beta \end{bmatrix} = \sqrt{\frac{2}{3}} \begin{bmatrix} 1 & -\frac{1}{2} & \frac{1}{2} \\ 0 & \frac{\sqrt{3}}{2} & -\frac{\sqrt{3}}{2} \end{bmatrix} \begin{bmatrix} i_a \\ i_b \\ i_c \end{bmatrix} \quad (5)$$

Park transformation:

$$\begin{bmatrix} i_d \\ i_q \end{bmatrix} = \begin{bmatrix} \cos\theta_e & \sin\theta_e \\ -\sin\theta_e & \cos\theta_e \end{bmatrix} \begin{bmatrix} i_\alpha \\ i_\alpha \end{bmatrix} \quad (6)$$

where i_d and i_q are the d-axis and q-axis current, respectively.

Mathematical model in the d–q axis:

$$\begin{cases} u_d = R_s i_d + L_d \dfrac{di_d}{dt} - \omega_e L_q i_q \\ u_d = R_s i_q + L_q \dfrac{di_q}{dt} - \omega_e L_d i_d + \omega_e \phi_f \end{cases} \quad (7)$$

where R_s is the winding resistance, and L_d and L_q are the d-axis and q-axis inductances, respectively.

The corresponding electromagnetic thrust equation in the d–q coordinate system can be simplified as:

$$F_e = \frac{3\pi P_n}{2\tau_n} \phi_f i_q + (L_q - L_d) i_d i_q \quad (8)$$

where P_n is the number of pole pairs.

SIMULATION MODEL

To verify the applicability and effectiveness of the established electromagnetic thrust model and its decoupling control strategy in the direct-drive heald frame system, this study constructs a simulation model of the direct-drive system tailored to the specific motion law of the heald frame within the MATLAB/Simulink simulation environment. The model comprehensively integrates the d-q axis decoupling control strategy, three-phase voltage model, electromagnetic thrust model, and the mechanical dynamic model of the heald frame, forming a complete closed-loop control system [19, 20]. The structure of the simulation model is shown in figure 2.

The heald frame's motion profile, defined by preset displacement and acceleration curves, simulates high-speed weaving dynamics and influences system thrust requirements. Using parameters from table 1, a realistic simulation model was built. Considering structural symmetry, each heald frame is driven by two direct-drive systems. Total masses of 5 kg, 10 kg, 15 kg, and 20 kg correspond to 2.5 kg, 5 kg, 7.5 kg, and 10 kg per system, respectively. This setup evaluates dynamic response and control robustness under varying loads.

Table 1

SIMULATION PARAMETERS			
Parameter Name	**Symbol**	**Value**	**Unit**
Stator resistance	R_s	0.5	Ω
d-axis inductance	L_d	26.7	mH
q-axis inductance	L_q	26.7	mH
Flux linkage	ϕ_f	0.24	W_b
Pole pitch	τ_n	20	mm
Number of pole pairs	p_n	6	—
Viscous damping coefficient	B	0.2	N·s/m^2

RESULTS AND DISCUSSION

Focusing on the modelling and simulation analysis of the direct-drive system tailored to the specific motion profile of the heald frame, this study presents a systematic study from multiple perspectives, including kinematic characteristics, load characteristics, current response, and electromagnetic thrust control.

Displacement, velocity, and acceleration analysis

In terms of kinematic characteristics, this study constructs the displacement function of the heald frame based on an 11th-order polynomial curve. The function was designed with full consideration of the smoothness and continuity requirements during the motion process. The displacement, velocity, and acceleration curves calculated using this polynomial function are shown in figure 3.

As illustrated in figure 3, the displacement profile follows a trapezoidal-like motion with rounded corners,

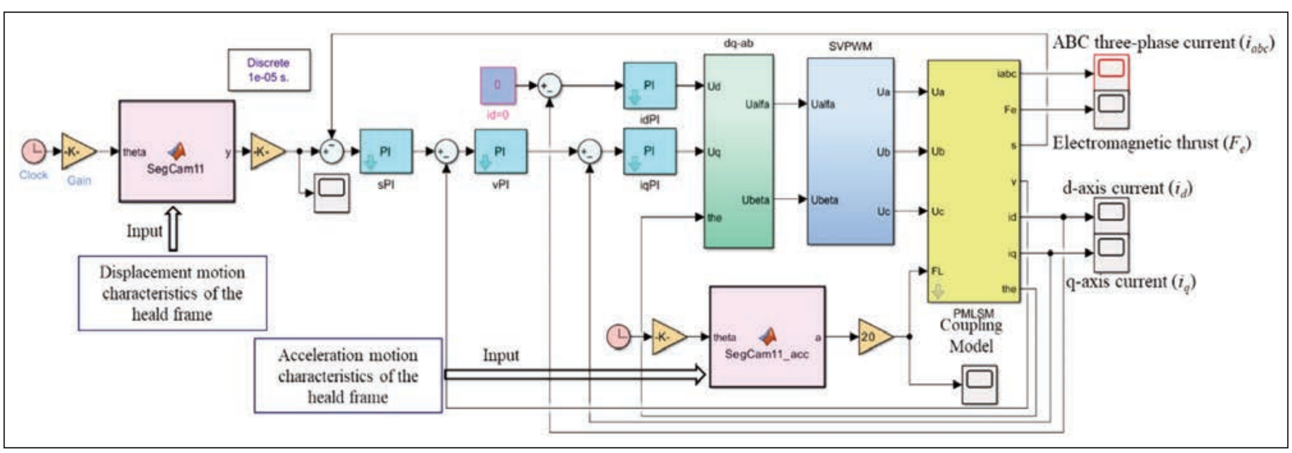

Fig. 2. Simulation modelling

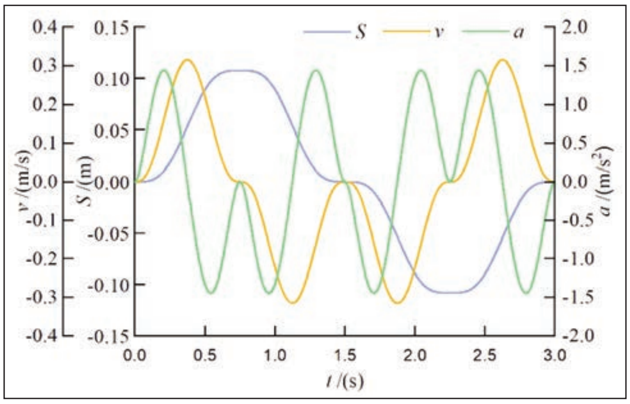

Fig. 3. Motion law of the heald frame

enabling rapid rise and fall while avoiding impulsive accelerations. The velocity curve is bell-shaped with zero initial and final values, satisfying the dwell requirements during the shedding process. Most importantly, the acceleration profile is continuous and differentiable, with no abrupt jumps, indicating C^2 continuity. Furthermore, the jerk remains bounded throughout the motion, achieving C^3 continuity; this is crucial for minimising excitation of structural resonances in the loom frame and preventing yarn breakage during high-frequency operation [21]. Compared to conventional fifth-order splines or modified sine profiles used in cam-based systems, the 11th-order polynomial offers greater tuning flexibility and superior dynamic performance.

Load analysis

In the modelling and simulation analysis of the direct-drive system tailored to the specific motion profile of the heald frame, load characteristics are one of the key indicators for evaluating system performance. By conducting simulation analysis on the acceleration of the heald frame under different mass conditions and combining this with the preset displacement trajectory, the variation of the load force experienced by the system during operation can be calculated, thereby obtaining the dynamic load response curve of the system, as shown in figure 4.

Figure 4 shows the load force curves under heald frame masses of 2.5 kg, 5 kg, 7.5 kg, and 10 kg,

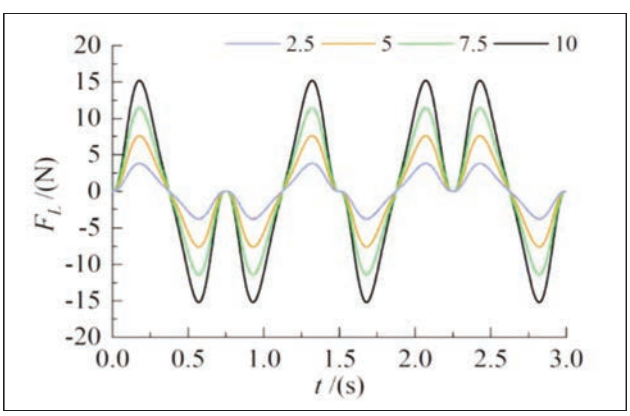

Fig. 4. Load variation law

exhibiting periodic fluctuations due to acceleration changes. The amplitude increases linearly with mass, reaching ±3.8 N, ±7.6 N, ±11.4 N, and ±15.2 N, respectively, verifying the theoretical model's accuracy. The observed linear scaling confirms Newtonian dynamics dominance; notably, F_L/m ≈ 1.52 m/s^2 matches the peak acceleration from the motion profile, validating kinematic-force consistency and enabling feedforward control for improved precision.

Current response

Figure 5 presents the current responses. The d-axis current (figure 5, *a*) remains near zero with minimal fluctuation, indicating effective field-oriented control and decoupling between magnetic field and thrust. The q-axis current (figure 5, *b*) increases linearly with mass, peaking at ±25 mA, ±45 mA, ±70 mA, and ±90 mA, respectively, showing the system's ability to regulate thrust dynamically. These results confirm the control system's fast response and high accuracy, laying a foundation for electromagnetic thrust optimisation and improved system stability.

Further analysis of figure 5, *b* shows that the q-axis current increases linearly with the heald frame's effective mass. At 2.5 kg, 5 kg, 7.5 kg, and 10 kg, the peak q-axis current values are approximately ±25 mA, ±45 mA, ±70 mA, and ±90 mA, respectively, indicating real-time current regulation to control electromagnetic thrust and ensure accurate displacement tracking, demonstrating the system's fast dynamic response and strong robustness under varying loads. As shown in figure 5, *c–e*, the three-phase currents (A, B, C) also increase linearly with the load, rising from ±20 mA at 2.5 kg to ±90 mA at 10 kg, maintaining symmetry and stability during steady-state operation. The sinusoidal waveform and phase symmetry reflect proper synchronisation with rotor position estimation, suggesting low harmonic distortion and efficient utilisation of DC bus power. The near-zero d-axis current confirms successful implementation of field-weakening avoidance and maximum thrust per ampere control, thereby maximising thrust output per unit current. These results validate the effectiveness of the d-q axis decoupling control strategy, enabling independent regulation of magnetic flux and thrust, significantly improving dynamic response and energy efficiency, and supporting long-term system reliability.

Driving force analysis

In the modelling and simulation analysis of the direct-drive system tailored to the specific motion laws of the heald frame, electromagnetic thrust, being the core parameter of the system's output control force, has dynamic response characteristics that directly determine the motion control performance of the heald frame under different external load conditions. Figure 6 shows the dynamic response curves of electromagnetic thrust under different effective masses of the heald frame (2.5 kg, 5 kg, 7.5 kg, and 10 kg), reflecting the variation trend of thrust output during startup and steady-state operation, as well as the system's adaptability to changes in external loads.

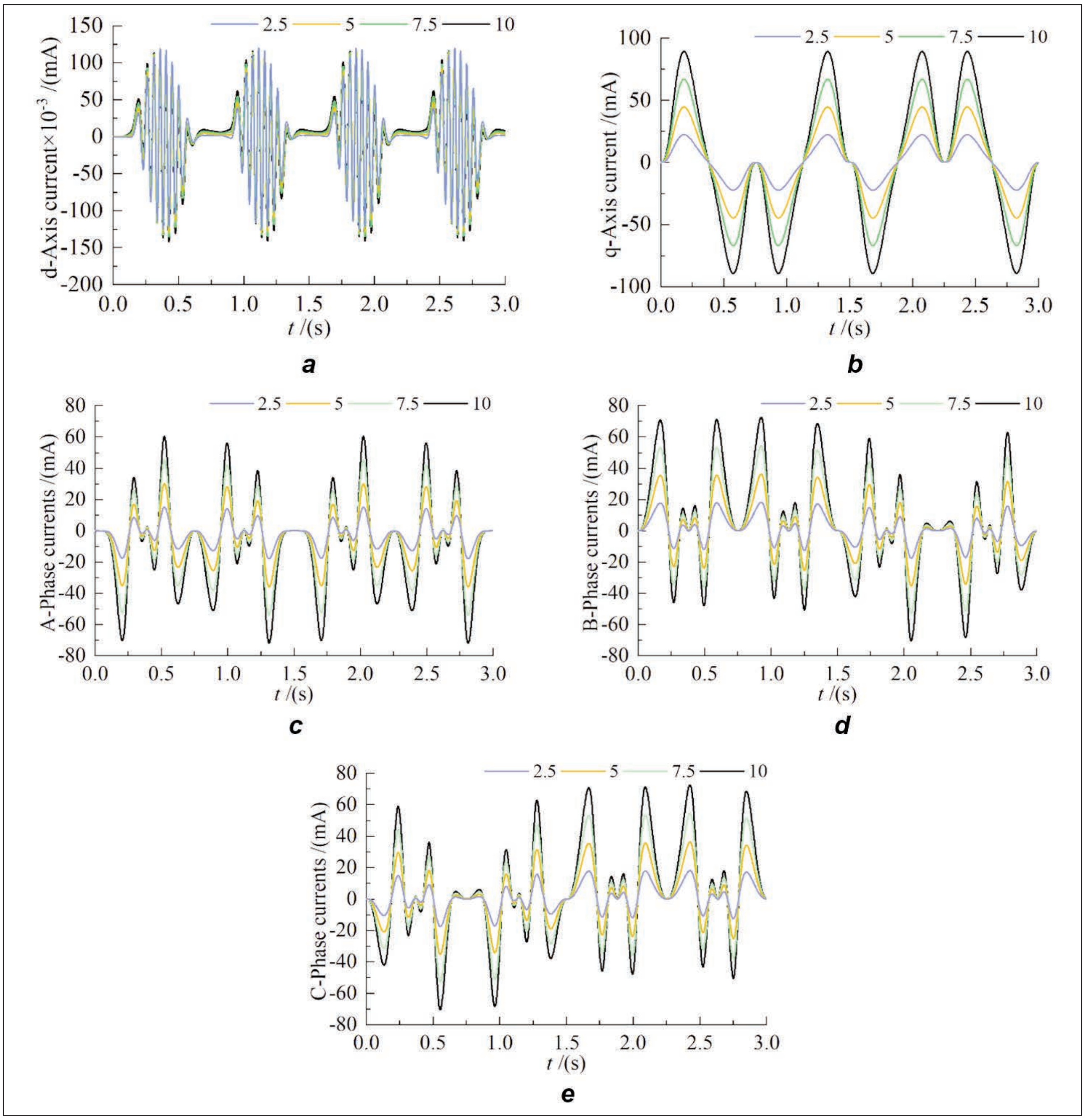

Fig. 5. Current results: *a* – d-Axis current; *b* – q-Axis current; *c* – Phase A current; *d* – Phase B current; *e* – Phase C current

As shown in figure 6, the electromagnetic thrust adaptively adjusts with load, increasing from ±7.6 N (2.5 kg) to ±30.3 N (10 kg), ensuring stable operation and precise displacement. The surplus thrust compensates for unmodeled disturbances like friction and misalignment, providing a safety margin for robust tracking. Although higher instantaneous power is required, the elimination of mechanical losses likely yields net energy savings. Thrust regulation correlates linearly with q-axis current, while near-zero d-axis current ensures effective decoupling, enhancing control efficiency and dynamic response.

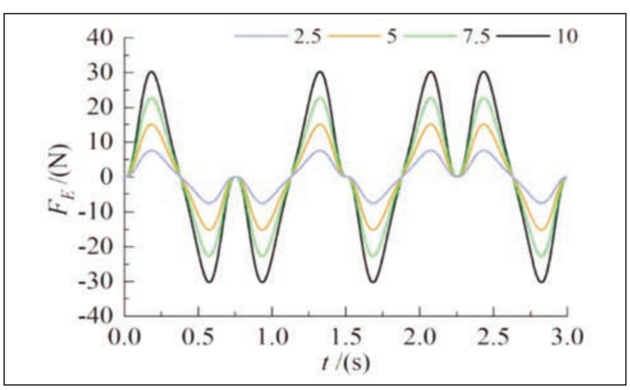

Fig. 6. Electromagnetic thrust results

CONCLUSIONS

This study focuses on modelling and simulating a direct-drive system for a loom heald frame using an 11th-order polynomial displacement function to ensure smooth motion profiles. A d-q axis mathematical model incorporating electromagnetic-mechanical coupling was established, and the Clark-Park transformation enabled decoupled control of flux linkage and thrust force. A closed-loop control system was simulated in MATLAB/Simulink under varying heald frame masses (2.5–10 kg) to evaluate dynamic performance. Results show fast response with no overshoot, stable and symmetrical three-phase currents, linear correlation between q-axis current and electromagnetic thrust, and near-zero d-axis current, confirming high control accuracy and system stability. The proposed direct-drive system demonstrates excellent dynamic performance and load adaptability. By eliminating mechanical transmission, it significantly reduces energy losses and maintenance requirements, extends service life, and lowers carbon emissions. Combined with high-efficiency electromagnetic actuation and the potential for regenerative braking in bidirectional operation, the system enhances energy recovery capability, aligning with the goals of green and intelligent manufacturing.

ACKNOLEDGEMENTS

The authors disclosed receipt of the following financial support for the research, authorship, and/or publication of this article: This research was financially supported by the Science and Technology Program of Tianjin Administration for Market Regulation (No. 2024-W43) and the National Key Research and Development Program (No. 2023YFC3081800). Thanks to partial support for this work from the Key Laboratory of Digital Twin Generic Technology in Special Equipment for State Market Regulation.

REFERENCES

[1] Jiang, J.B., Wei, C., Yu, Y.F., Sun, S.X., *Autonomous planning of discontinuous terrain-dependent crawling for space dobby robots,* In: Sensors, 2023, 23, 6, 3334, https://doi.org/10.3390/s23063334

[2] Kolčavová, B., Tunakova, V., Tunák, M., Jezik, K., *Influence of woven fabric construction parameters on electromagnetic shielding effectiveness: Part I – weave influence*, In: Textile Research Journal, 2022, 92, 21–22, 004051752211003, https://doi.org/10.1177/00405175221100390

[3] Wang, S., Yan, Z.J., Shen, F., Du, L.H., Li, G.L., Yang, Q., Hu, Q.H., *Novel aptasensor based on polyaniline functionalized carboxylated dobby carbon nanotubes and molybdenum disulfide for endotoxin detection,* In: Talanta, 2024, 276, 126256, https://doi.org/10.1016/j.talanta.2024.126256

[4] Yu, H.B., Yin, H.H., Peng, J.Q., Wang, L., *Comparison of the vibration response of a rotary dobby with cam-link and cam-slider modulators*, In: Autex Research Journal, 2021, 21, 4, 491–500, https://doi.org/10.2478/aut-2020-0037

[5] Qiu, H., Han, B., Huang, P.F., Zhang, H.W., *Structural design and dynamics optimization for heald frame made by carbon fiber reinforced composites*, In: Journal of Industrial Textiles, 2022, 52, 8, 252699082, https://doi.org/10.1177/15280837221130514

[6] Iftekhar, H., Umair, M., Hamdani, S.T.A., Imran, S.M., *Effect of hybrid weave patterns on the mechanical performance of woven fabrics*, In: Journal of Natural Fibers, 2022, 20, 1, 2145411, https://doi.org/10.1080/15440478.2022.2145411

[7] Li, L.Q., Fang, Y.F., Wang L., *Design of a family of multi-DOF drive systems for fewer limb parallel mechanisms*, In: Mechanism and Machine Theory, 2020, 148, 94–114, https://doi.org/10.1016/j.mechmachtheory.2020.103802

[8] Yoshida, T., *A method for approximating weave diagrams under heald frame constraint*, In: Textile Research Journal, 2023, 93, 15–16, 3527–3537, https://doi.org/10.1177/00405175221149684

[9] Sirkova, B.K., Mertova, I., *Prediction of warp and weft crimp in the construction of dobby woven fabrics, In:* Journal of the Textile Institute, 2020, 111, 10, 1401–1409, https://doi.org/10.1080/00405000.2019.1701967

[10] Hassan, M., Mostafa, A., Al-Oufy, A., El-Gholmy, S., *Numerical investigation of weaving machine heald shaft new design using composite material to improve its performance*, In: Autex Research Journal, 2024, 24, 01, 1–11, https://doi.org/10.1515/aut-2023-0026

[11] Cho, K., Kim, J., Choi, S.B., Oh, S., *A high-precision motion control based on a periodic adaptive disturbance observer in a PMLSM*, In: IEEE/ASME Transactions on Mechatronics, 2015, 20, 5, 2158–2171, https://doi.org/10.1109/TMECH.2014.2365996

[12] Ullah, N., Basit, A., Khan, F., Shah, Y.A., Khan, A., Waheed, O., *Design and optimization of complementary field excited linear flux switching machine with unequal primary tooth width and segmented secondary*, In: IEEE Access, 2019, 7, 106359–106371, https://doi.org/10.1109/ACCESS.2019.2932791

[13] Tan, Q., Wang, M.Y., Li, L.Y., Li, J.C., *Research on Non-integer pole number for segmental permanent magnet linear synchronous motor*, In: IEEE Transactions on Industrial Electronics, 2021, 68, 5, 4120–4130, https://doi.org/10.1109/TIE.2020.2985001

[14] Huang, X.Z., Yu, H.C., Zhou, B., Li, L.Y., Gerada, D., Gerada, C., *Detent-force minimization of double-sided permanent magnet linear synchronous motor by shifting one of the primary components*. In: IEEE Transactions on Industrial Electronics, 2020, 67, 1, 180–191, https://doi.org/10.1109/TIE.2019.2892704

[15] Tan, Z.X., Liu, L., Li, Y.J., He, F., Liu, B.Y., Yi, Z.X., *A Robust Model Predictive Current Control Strategy with Improved Adaptive Quantum Genetic Algorithm-Based Parameter Identification for PMSM*, In: IEEE Transactions on Energy Conversion, 2025, 1–11, https://doi.org/10.1109/TEC.2025.3596340

[16] Zeng, Z.Q., Lu, Q.F., *Investigation of novel partitioned-primary hybrid-excited flux-switching linear machines*, In: IEEE Transactions on Industrial Electronics, 2018, 65, 12, 9804–9813, https://doi.org/10.1109/TIE.2017.2786205

[17] Li, T., Sun, X.D., Lei, G., Guo, Y.G., Yang, Z.B., Zhu, J.G. *Finite-control-set model predictive control of permanent magnet synchronous motor Drive systems – an overview*, In: IEEE/CAA Journal of Automatica Sinica, 2022, 9, 12, 2087–2105, https://doi.org/10.1109/JAS.2022.105851

[18] Peng, J., Yao, M., *Overview of predictive control technology for permanent magnet synchronous motor systems*, In: Applied Sciences, 2023, 13, 10, 6255, https://doi.org/10.3390/app13106255

[19] Hazzab, A, Bousserhane, I.K., Zerbo, M., Sicard, P., *Real time implementation of fuzzy gain scheduling of PI controller for induction motor machine control*, In: Neural Processing Letters, 2006, 24, 3, 203–215, https://doi.org/10.1007/s11063-006-9018-5

[20] Sant, A.V., Rajagopal, K.R., Sheth, N.K., *Permanent magnet synchronous motor drive using hybrid PI speed controller with inherent and noninherent switching functions*, In: IEEE Transactions on Magnetics, 2011, 47, 10, 4088–4091, https://doi.org/10.1109/TMAG.2011.2159831

[21] Liao, C.S., Jeng, S.L., Chieng, W.H., *Electronic cam motion generation with special reference to constrained velocity, acceleration, and jerk*, In: ISA Transactions, 2004, 43, 3: 427–443, https://doi.org/10.1016/S0019-0578(07)60159-1

Authors:

QINGYUAN GUO[1,2], TAO YANG[3], SIJIA FU[4], HONGBIN YU[3]

[1]School of Electronics and Information Engineering, Tiangong University, Tianjin 300387, China
e-mail: 2320080144@tiangong.edu.cn

[2]Key Laboratory of Digital Twin Generic Technology in Special Equipment for State Market Regulation, Tianjin Special Equipment Inspection Institute, Tianjin 300192, China

[3]School of Mechanical Engineering, Tiangong University, Tianjin 300387, China
e-mail: yangtao@tiangong.edu.cn

[4]Japan Electronics College, Tokyo 169-0073, Japan
e-mail: holymelon0000@163.com

Corresponding author:

HONGBIN YU
e-mail: yuhongbin@tiangong.edu.cn